Towards efficient tin-doped indium oxide (ITO)-free inverted organic solar cells using metal cathodes

J. Meiss,[a] M. K. Riede, and K. Leo
Institut für Angewandte Photophysik, Technische Universität Dresden, D-01062 Dresden, Germany

(Received 24 October 2008; accepted 9 December 2008; published online 7 January 2009)

We present zinc phthalocyanine (ZnPc):C_{60} bulk-heterojunction top-illuminated organic solar cells using ultrathin metal layers as transparent top contacts. We show that solar cell performance sensitively depends on the interface and morphology of the cathode, which can be influenced by varying the composition and layer structure of the metal contact. We investigate various metal combinations, such as 3 nm Al/8 nm Ag and 7 nm Al/14 nm Ag, to illustrate the necessity to find a suitable combination of morphology and electrical and optical properties. Solar cells using standard materials and a 1 nm Al/14 nm Ag cathode exhibit promising efficiencies of over 2.2%.
© *2009 American Institute of Physics*. [DOI: 10.1063/1.3059552]

As a potential alternative to expensive silicon solar cells, organic solar cells (OSCs) got into the focus of research interest in the last years.[1,2] OSCs are currently particularly interesting for niche markets where cost-efficient, lightweight, and flexible solutions are advantageous.

A widely recognized issue in the context of thin-film optoelectronic devices is the standard transparent conductive substrate, indium tin oxide (ITO). While this material provides an excellent combination of transparency and conductivity, it is also brittle[3] (inhibiting its use in flexible devices) and expensive. If inverted devices are to be fabricated, ITO is not suitable since sputtering onto organic layers damages the layers underneath. The same issue arises when replacing ITO with other transparent conductive oxides (TCOs). Generally, increasing effort is being given to find alternative transparent conductive materials, e.g., carbon nanotubes for polymer-based solar cells,[4] conductive polymers,[5,6] metals,[7,8] or solution-processed nanowire mesh arrays.[9]

In this paper, TCO-free top-illuminated small-molecule OSCs deposited on a nonopaque anode are presented. As semitransparent contacts, they employ different thin-film metal systems. It is demonstrated that multilayer metal contacts are a feasible alternative electrode with good processibility. Solar cells using the ZnPc:C_{60} absorber system and a 1 nm Al/14 nm Ag cathode exhibit promising efficiencies of over 2.2%.

The solar cells are fabricated in a custom-made vacuum system (K.J. Lesker, UK) at a base pressure of 10^{-6} mbar using shadow masks. Float glass cleaned with organic solvents is used as substrate. A metal back contact of 100 nm Al is deposited, followed by 1 nm of a proprietary *p*-type dopant (Novaled AG, Dresden, Germany).[10] As hole transporting material, 30 nm of 10 wt % *p*-doped 4,4′,4″-tris(1-naphthylphenylamino)-triphenylamine is used. For light absorption, a layer of zinc phthalocyanine (ZnPc) (10 nm), followed by a layer of coevaporated ZnPc:C_{60} (25 nm, ratio of 1:1) are deposited. After an additional absorber and transport layer of C_{60} (40 nm), 7 nm of 4,7-diphenyl-1,10-phenanthroline (BPhen) is used as exciton blocker. Different thicknesses and combinations of Al/Ag (9–21 nm total thickness) are used as transparent top contact. A 60 nm capping layer of tris(8-hydroxy-quinolinato)-aluminum (Alq_3) is used for increased light outcoupling out of the solar cell.[8] All organic materials have been purified at least twice by vacuum gradient sublimation.

A total of 16 samples are made on the same substrate in one run. This way, the only variations are for the top contact while keeping the deposition conditions for all other layers (hole transport layer, absorber, electron transport layer, and capping layer) constant. Typical solar cell areas are around 6.7 mm^2, measured using a light microscope.

The completed solar cells are encapsulated in a nitrogen glovebox attached to the vacuum deposition chamber, then stored at ambient conditions. $J(V)$-characteristics are recorded using a source measurement unit 236 SMU (Keithley) under an AM 1.5G sun simulator (Hoenle AG), monitored with a silicon photodiode with respect to which intensities are given. The $J(V)$-characteristics are not corrected for spectral mismatch. External quantum efficiency (EQE) is measured in the same setup using color filters. Measurements with different illumination intensities are performed with neutral density filters. Reflection and transmission are measured on a Lambda 900 UV/visible/near infrared spectrometer (PerkinElmer).

The obtained solar cell characteristics for different metal contacts consisting of variations in aluminum (1–7 nm) and silver (8–14 nm) in different combinations are summarized in Table I. All short-circuit currents given are normalized to an incident light intensity of 100 mW/cm^2. Values of OSC with 5 nm Al cathodes are omitted due to space constraints. While there are some deviations due to experimental scatter, it can be seen that the composition and layer thickness of the transparent top contact have significant influence on the overall device performance and exhibit clear trends. Three main factors can be distinguished: the thickness of Al, the thickness of Ag, and the overall metal thickness of Al/Ag combined.

The thickness of the Al layer is varied between 1 and 7 nm. As found in a previous study,[8] the addition of Al to the cathode alone can lead to a significant improvement, presumably due to surfactant effects that lead to more closed Ag layers and prevent cluster formation compared to stand-alone pure Ag layers. Previous studies[11] showed that less reactive

[a]Electronic mail: jan.meiss@iapp.de.

 © 2009 American Institute of Physics

Downloaded 10 Jan 2010 to 141.30.25.195. Redistribution subject to AIP license or copyright; see http://apl.aip.org/apl/copyright.jsp

TABLE I. Solar cell characteristics.

Metal contact	J_{sc} (mA/cm^2)	V_{oc} (V)	FA (%)	η (%)
1 nm Al, 8 nm Ag	0.01	0.525	N/A	N/A
1 nm Al, 10 nm Ag	3.26	0.503	13.45	0.22
1 nm Al, 12 nm Ag	7.42	0.520	52.17	2.01
1 nm Al, 14 nm Ag	7.90	0.519	53.86	2.21
3 nm Al, 8 nm Ag	6.14	0.515	29.53	0.93
3 nm Al, 10 nm Ag	5.95	0.516	52.14	1.71
3 nm Al, 12 nm Ag	6.49	0.512	52.64	1.49
3 nm Al, 14 nm Ag	6.57	0.514	52.52	1.92
7 nm Al, 8 nm Ag	4.55	0.503	57.56	1.43
7 nm Al, 10 nm Ag	4.73	0.508	55.69	1.34
7 nm Al, 12 nm Ag	4.74	0.516	57.50	1.40
7 nm Al, 14 nm Ag	4.92	0.504	60.59	1.39

metals such as Ni and Cu can form metallic precipitates within polyimide layers without reacting, while Cr reacted with the organic material and was bound to its surface forming continuous layers. This suggests that the Al layers presented in this paper can also react with BPhen and form a smooth surface on which the Ag can then adhere in closed flat layers. Noble metals alone, such as Ag, Au, and Pt, on the contrary, tend to diffuse and form clusters even on crystalline organic materials at room temperature.[12]

As can be seen from the data shown here, an increase in Al thickness leads to a clear decrease in the short-circuit current J_{sc}, which can be explained by higher reflection of Al in the ranges of 400–500 nm and 600–700 nm, decreasing the photon density in the absorber and inhibiting exciton generation. This is illustrated in the reflection measurements shown in the inset of Fig. 1, where the lowest reflection values are obtained for a metal electrode having only 1 nm Al and a total thickness of 15 nm.

Note that the reflection is high, especially in the 400–600 nm range. The values shown in Fig. 1, however, characterize a sample without Alq_3 capping layer, which considerably reduces reflection and at the same time utilizes the metal reflection to create a microcavity effect within the OSC for improved performance.[8]

The electrode with 3 nm Al and a total thickness of only 11 nm exhibits higher reflection, showing that the main contribution toward reflection stems from the Al content. These

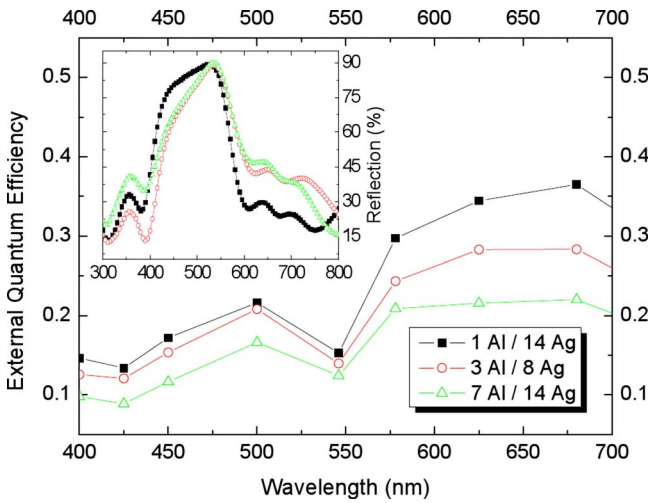

FIG. 1. (Color online) EQE measurements. Inset: reflection measurements. Filled squares: 1 nm Al/14 nm Ag. Empty circles: 3 nm Al/8 nm Ag. Empty triangles: 7 nm Al/14 nm Ag.

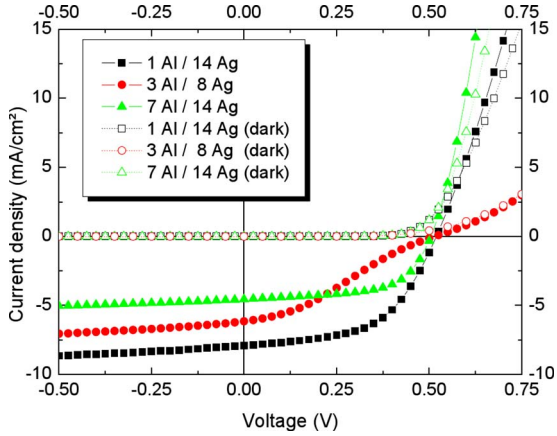

FIG. 2. (Color online) Current-voltage curves with AM 1.5G and without illumination. Filled symbols: under illumination. Empty symbols: in the dark. Squares: 1 nm Al/14 nm Ag. Circles: 3 nm Al/8 nm Ag. Triangles: 7 nm Al/14 nm Ag.

findings are supported by EQE measurements shown in Fig. 1, where in particular the EQE in the 600–700 nm range drops from 35% to almost 20% upon increasing the Al thickness. This coincides with the main ZnPc absorption range, leading to lower photocurrents with increasing Al thickness. Highest currents are obtained with 1 nm Al with currents of up to 7.9 mA/cm^2, which drops to 6–6.6 mA/cm^2 for 3 nm Al, 5.5–5.7 mA/cm^2 for 5 nm Al, and reaches a minimum for 7 nm Al with 4.6–4.9 mA/cm^2. Thicker Al layers seem to slightly reduce the open-circuit voltage (V_{oc}) from 0.52 V for 1 nm Al to 0.51 V for 7 nm Al with decreasing voltage for increasing Al thickness. It is currently not clear if this effect is caused by different work functions of Ag (4.26 eV) and Al (4.28 eV) (values reported by Michaelson[13]), or possibly the diffusion of Al atoms into adjacent organic layers of BPhen and C_{60}, which might lead to unintentional doping. These negative effects are partially compensated by an improvement of the fill factor (FF) for thicker layers. However, since an increase in FF can also be observed for increasing Ag layer thickness, this superposition of influences makes it difficult to evaluate the proportions of the contributions of both materials to FF. Generally it can be seen that thicker Al layers are disadvantageous to solar cell performance, mainly due to negative optical properties.

In the current work, silver has been used as the main conductive component for the metal electrodes due to its advantageous optical properties. Ultrathin Ag films are very sensitive to deposition conditions, and for thin metal films it is assumed that uniform films are found only at thicknesses above a certain coalescence threshold, depending on evaporation rate, substrate, pressure, etc.[14] With an Al base layer, the morphological features of the Ag layer less likely inhibit an optimal contact because the Al seems to act as surfactant, mediating smooth Ag morphology.

For the solar cells with 1 nm Al/8 nm Ag, it is assumed that the amount of silver is too small for a closed layer, despite the 1 nm Al deposition. While a small photovoltage is observed, the measured efficiency is in the low 10^{-3}% range and is considered negligible.

Examples of selected $J(V)$-characteristics under illumination and in the dark are shown in Fig. 2. Fully operational solar cells are obtained with 3 nm Al/8 nm Ag, having J_{sc} =6.1 mA/cm^2 and V_{oc}=0.52 V, which is in the same range

Downloaded 10 Jan 2010 to 141.30.25.195. Redistribution subject to AIP license or copyright; see http://apl.aip.org/apl/copyright.jsp

as the characteristics of other solar cells, albeit having a lower FF below 30%. The creation of an operational solar cell suggests that well-defined closed layers are indeed possible even with thicknesses of individual metal films below 10 nm.

The solar cell with 7 nm Al/14 nm Ag has the thickest metal contact of all devices presented in this study. Due to its lower transmission (especially caused by the 7 nm Al), the photocurrent is low with 4.9 mA/cm^2. This is more than compensated for by the high FF of over 60%, leading to an overall increase in efficiency to 1.39% from 0.93%, which is found for the 3 nm Al/8 nm Ag contact, despite considerably lower quantum efficiency. This is expected to originate from a superior electrical contact between the organic/metal interface and an increased number of charge carrier percolation pathways within the metal contact. This is reflected in a lower series resistance for voltages $>V_{oc}$ as can be observed in the slope of the $J(V)$-curves under illumination and in the dark. In both cases, the sample having 7 nm Al/14 nm Ag has the lowest series resistance and, as suggested in the saturation behavior, the highest parallel resistance, indicating good electrical contact and low leakage current. In contrast, the thin metal contact of 3 nm Al/8 nm Ag exhibits the highest series and lowest parallel resistance. The low FF and the visible "S-kink" hint at issues in charge extraction, or high recombination. This can be caused by the Ag layer, which is thick enough for electrical contact, but still has some isolated clusters, islands, or hillocks that act as charge carrier traps for electrons, leading to unbalanced charge carrier extraction and creating a counterfield. It cannot be excluded that the noncontinuous Ag layer allows residual oxygen to penetrate Al, leading to Al_2O_3.

The best solar cell of the current study has a combination of 1 nm Al, preserving high transmission while at the same time acting as a surface-mediating layer, and 14 nm Ag for a closed layer with only few clusters. This configuration yields the best compromise of $J_{sc}=7.90$ mA/cm^2 and FF=54%, leading to an overall efficiency of over 2.2%. It is expected that this metal contact can be used in an optimized solar cell stack with different transport materials or absorbers to achieve considerably higher performance.

Neutral density filter measurements are performed to further investigate the effects of the metal contact for different illumination intensities. The effect of incident light intensity on FF and V_{oc} is shown in Fig. 3, where the thinnest (3 nm Al/8 nm Ag) and thickest (7 nm Al/14 nm Ag) solar cells are chosen. V_{oc} shows an exponential increase for increasing illumination for both contact types, as is expected when the quasi-Fermi–Niveau splitting becomes more pronounced due to higher charge carrier generation.

A clear difference is visible for the FF. While the solar cell with the thick metal contact shows an exponential increase with a saturationlike behavior, the thin metal electrode leads to a peak at 0.025 suns, followed by decreasing FF values. This suggests an increasing influence of the series resistance at higher photogenerated currents and higher recombination due to hindered charge carrier extraction through an insufficiently formed percolation network.

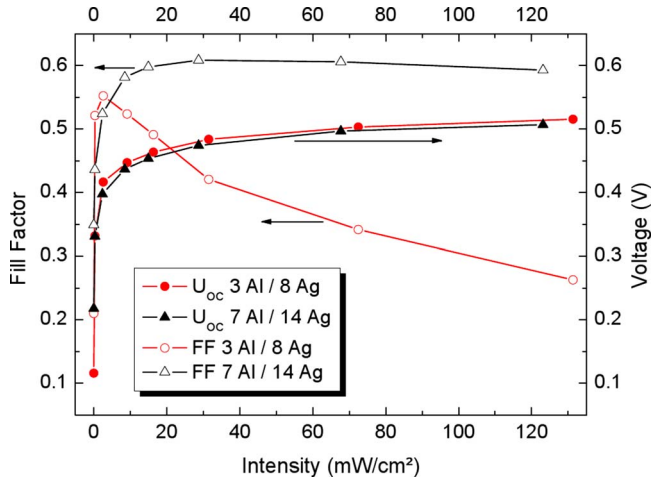

FIG. 3. (Color online) Intensity-dependent FF and open-circuit voltage (V_{oc}). Right scale: V_{oc} of solar cells with 3 nm Al/8 nm Ag (filled circles) and 7 nm Al/14 nm Ag (filled triangles) contacts. Left scale: FF of solar cells with 3 nm Al/8 nm Ag (empty circles) and 7 nm Al/14 nm Ag (empty triangles) contacts. The lines are guide to the eyes.

In summary, ITO-free inverted organic bulk heterojunction solar cells with cathodes from thermally evaporated combinations of ultrathin Al and Ag films are presented. It is shown that despite better optical properties, too thin metal cathodes are inferior under operation due to isolated clusters and remaining islands that lower FF. The optimal solar cell structure employs a combination of 1 nm Al for improved morphology of the metal contact and 14 nm Ag for improved electrical and optical properties, and reaches promising efficiencies of over 2.2%, which is expected to increase further by optimization of solar cell stack and used materials.

The current work is supported by the Bundesministerium für Bildung und Forschung (Project No. 03IP602).

[1]C. W. Tang, Appl. Phys. Lett. **48**, 183 (1986).
[2]J. Xue, S. Uchida, B. P. Rand, and S. R. Forrest, Appl. Phys. Lett. **85**, 5757 (2004).
[3]Z. Chen, B. Cotterell, W. Wang, E. Guenther, and S.-J. Chua, Thin Solid Films **394**, 201 (2001).
[4]J. van de Lagemaat, T. M. Barnes, G. Rumbles, S. E. Shaneen, T. J. Coutts, C. Weeks, I. Levitsky, J. Peltola, and P. Glatkowsky, Appl. Phys. Lett. **88**, 233503 (2006).
[5]J. Meiss, C. L. Uhrich, K. Fehse, S. Pfuetzner, M. K. Riede, and K. Leo, Proc. SPIE **7002**, 700210 (2008).
[6]B. Zimmermann, M. Glatthaar, M. Niggemann, M. K. Riede, A. Hinsch, and A. Gombert, Sol. Energy Mater. Sol. Cells **91**, 374 (2007).
[7]T. Oyamada, Y. Sugawara, Y. Terao, H. Sasabe, and C. Adachi, Jpn. J. Appl. Phys., Part 1 **46**, 1734 (2007).
[8]J. Meiss, N. Allinger, M. K. Riede, and K. Leo, Appl. Phys. Lett. **93**, 103311 (2008).
[9]J.-Y. Lee, S. T. Connor, Y. Cui, and P. Peumans, Nano Lett. **8**, 689 (2008).
[10]Used for better processibility, comparable in performance to the commonly available 2,3,5,6-tetrafluoro-7,7,8,8-tetracyanoquinodimethane.
[11]F. K. LeGoues, B. D. Silverman, and P. S. Ho, J. Vac. Sci. Technol. A **6**, 2200 (1988).
[12]A. E. Duerr, F. Schreiber, M. Kelsch, H. D. Carstanjen, and H. Dosch, Adv. Mater. (Weinheim, Ger.) **14**, 961 (2002).
[13]H. B. Michaelson, J. Appl. Phys. **48**, 4729 (1977).
[14]R. S. Sennett and G. D. Scott, J. Opt. Soc. Am. **40**, 203 (1950).

Downloaded 10 Jan 2010 to 141.30.25.195. Redistribution subject to AIP license or copyright; see http://apl.aip.org/apl/copyright.jsp